Quasielastic neutron scattering study of hydrogen motion in C14- and C15-type $ZrCr_2H_x$

1999 J. Phys.: Condens. Matter 11 1489

(http://iopscience.iop.org/0953-8984/11/6/013)

J. Phys.: Condens. Matter **11** (1999) 1489–1502. Printed in the UK PII: S0953-8984(99)98637-X

Quasielastic neutron scattering study of hydrogen motion in C14- and C15-type $ZrCr_2H_x$

A V Skripov†, M Pionke‡, O Randl§¶ and R Hempelmann‖

† Institute of Metal Physics, Urals Branch of the Academy of Sciences, Ekaterinburg 620219, Russia
‡ Institut für Festkörperforschung, Forschungszentrum Jülich, D-52425 Jülich, Germany
§ Institut Laue–Langevin, F-38042 Grenoble, France
‖ Institut für Physikalische Chemie, Universität des Saarlandes, D-66041 Saarbrücken, Germany

Received 23 October 1998

Abstract. In order to clarify the mechanisms of hydrogen diffusion in the cubic (C15) and hexagonal (C14) modifications of Laves phase $ZrCr_2$, we have performed high-resolution quasielastic neutron scattering measurements on C15-$ZrCr_2H_{0.45}$ and C14-$ZrCr_2H_{0.5}$ over the temperature range 10–340 K. It is found that in both systems the diffusive motion of hydrogen can be described in terms of two jump processes: the fast localized H motion within the hexagons formed by interstitial (Zr_2Cr_2) sites and the slower hopping from one hexagon to the other. The experimental results are analysed to determine the hydrogen hopping rates and the tracer diffusion coefficients as functions of temperature. The motional parameters of hydrogen in the C15- and C14-type samples are found to be close to each other. Comparison of the motional parameters of hydrogen in $ZrCr_2H_x$ and in the related C15-type TaV_2H_x shows that the localized H motion in $ZrCr_2$ is slower, whereas the long-range H diffusion is much faster than in TaV_2. These features are consistent with the difference between intersite distances in the hydrogen sublattices of $ZrCr_2H_x$ and TaV_2H_x.

1. Introduction

The Laves-phase intermetallic compound $ZrCr_2$ may exist in the form of either of two structural modifications (the hexagonal C14 or the cubic C15), both of which absorb large amounts of hydrogen. Nuclear magnetic resonance (NMR) experiments [1–3] have revealed the extremely high hydrogen mobility down to low temperatures in both C14- and C15-type $ZrCr_2H_x$ with $x \leqslant 0.5$. In particular, the long-range hydrogen diffusivity D in these compounds at 130 K appears to be higher than in any other intermetallic–hydrogen system. However, the mechanisms of H motion in $ZrCr_2H_x$ are not yet clear. The temperature dependence of D in both C14- and C15-type $ZrCr_2H_x$ measured by the pulsed-field-gradient NMR technique [3] shows a pronounced deviation from the Arrhenius behaviour below 200 K. Furthermore, the proton spin-relaxation results for $ZrCr_2H_x$ [2] are consistent with a coexistence of two frequency scales of H hopping. Similar coexistence of two frequency scales of H hopping has been reported for a number of other Laves phase hydrides including $TiCr_2H_x$ [4], TaV_2H_x [5], HfV_2H_x and ZrV_2H_x [6]. Recent quasielastic neutron scattering (QENS) measurements on C15-type TaV_2H_x [7–9] have shown that the diffusive motion of hydrogen in this system can

¶ Present address: Michelin SA, Place des Carmes, F-63040 Clermont-Ferrand, France.

0953-8984/99/061489+14$19.50

be described in terms of two jump processes: the fast localized H motion within hexagons formed by interstitial g (Ta_2V_2) sites and the slower hopping from one hexagon to the other.

According to the neutron diffraction data [10, 11], hydrogen atoms in C15-type $ZrCr_2H_x$ with $x \leqslant 3.5$ also occupy only tetrahedral g (Zr_2Cr_2) sites. Therefore one can expect the microscopic picture of hydrogen motion in C15-$ZrCr_2H_x$ with low x to be qualitatively the same as that for TaV_2H_x. For C14-$ZrCr_2H_x$ no published information on positions occupied by H atoms is available. However, on the basis of the general trends of site occupancy in hydrides of intermetallics [12, 13] and the neutron diffraction data for the related system C14-$ZrMn_2D_3$ [14], we may expect hydrogen in C14-$ZrCr_2H_x$ to occupy the tetrahedral sites with (Zr_2Cr_2) coordination, at least at low x. In contrast to the C15 structure, where all (Zr_2Cr_2) sites are equivalent, in the C14 structure there are four inequivalent types of (Zr_2Cr_2) site (h_1, h_2, k and l). The spatial arrangement of (Zr_2Cr_2) sites in the C14 lattice differs from that in the C15 lattice. The aims of the present work are to clarify the microscopic picture of H hopping in both C14- and C15-type $ZrCr_2$ and to compare the motional parameters of hydrogen in C14- and C15-type compounds of the same composition using incoherent quasielastic neutron scattering. We have performed high-resolution QENS measurements for C15-$ZrCr_2H_{0.45}$ and C14-$ZrCr_2H_{0.5}$ over the temperature range 10–340 K. These measurements have confirmed the existence of a fast localized H motion (similar to that found for TaV_2H_x) in both C14- and C15-type $ZrCr_2H_x$. The results are analysed to determine the tracer diffusion coefficient, the hopping rates and the mean jump length of hydrogen atoms in $ZrCr_2$.

2. Experimental details

The preparation of $ZrCr_2H_x$ samples was analogous to that described in [1, 2]. X-ray diffraction analysis has shown that both C15-$ZrCr_2H_{0.45}$ and C14-$ZrCr_2H_{0.5}$ are single-phase solid solutions with the lattice parameters $a_0 = 7.26$ Å (C15) and $a_0 = 5.15$ Å, $c_0 = 8.42$ Å (C14).

QENS measurements were performed on the high-resolution backscattering spectrometers IN10 (Institut Laue–Langevin, Grenoble) and BSS1 (Forschungszentrum Jülich). Both spectrometers use the Si(111) monochromator and analysers selecting the neutron wavelength $\lambda = 6.271$ Å. The ranges of energy transfer $\hbar\omega$ in our experiments were ± 13.6 μeV (IN10) and ± 15.2 μeV (BSS1), the FWHM energy resolutions being 0.9 and 1.2 μeV, respectively. The ranges of momentum transfer $\hbar Q$ studied corresponded to Q-ranges of 0.41–1.94 Å^{-1} (IN10) and 0.16–1.88 Å^{-1} (BSS1).

The powdered $ZrCr_2H_x$ samples were placed into flat Al containers with a depth of 1 mm. In the experiments on both spectrometers the plane of the container was oriented along the direction $2\theta \approx 97^\circ$. This direction corresponds to the only Bragg reflection (in the Q-range studied) for the C15 sample and to one of three low-Q Bragg reflections for the C14 sample. In order to avoid Bragg reflections, the analyser plate surfaces were partially shielded by cadmium. For C15-$ZrCr_2H_{0.45}$ the QENS spectra were recorded using both IN10 (at the temperatures 10, 140, 150, 160, 170, 215, 239, 264 and 293 K) and BSS1 (14, 130, 200, 230, 260, 300 and 340 K). The C14-$ZrCr_2H_{0.5}$ sample was studied only on IN10 at the temperatures 10, 128, 140, 155, 173, 210, 234, 259, 279 and 303 K. The raw experimental data were corrected for absorption and self-shielding using the standard ILL programs. The value of the transmission coefficient measured for C15-$ZrCr_2H_{0.45}$ at room temperature was 0.93 ± 0.02.

For both spectrometers the instrumental resolution functions were determined from the QENS spectra of $ZrCr_2H_x$ at low temperatures (10 K for IN10 and 14 K for BSS1). The background spectra were measured for the identical outgassed C15-$ZrCr_2$ sample at 293 K in the same experimental geometry as for $ZrCr_2H_x$. The scattering function $S_{\mathrm{exp}}(Q, \omega)$ of the hydrogen sublattice was determined by subtracting these background spectra from the $ZrCr_2H_x$ spectra.

3. Results and discussion

3.1. QENS spectra: an overview

The experimental QENS spectra for C15-$ZrCr_2H_{0.45}$ and C14-$ZrCr_2H_{0.5}$ show qualitatively similar behaviour over the temperature range studied. Between 128 and 173 K the spectra can be satisfactorily described by a sum of two components: a narrow 'elastic' line represented by the spectrometer resolution function $R(Q, \omega)$ and a resolution-broadened Lorentzian 'quasielastic' line. As an example of the data, figure 1 shows the QENS spectrum of C15-$ZrCr_2H_{0.45}$ recorded at 170 K for $Q = 1.94$ Å. As the first step of the analysis, we have fitted $S_{\mathrm{exp}}(Q, \omega)$ with the model incoherent scattering function

$$S_{\mathrm{inc}}(Q, \omega) = A_0(Q)\delta(\omega) + [1 - A_0(Q)]L(\omega, \Gamma) \tag{1}$$

convoluted with $R(Q, \omega)$. Here $\delta(\omega)$ is the 'elastic' δ-function, $L(\omega, \Gamma)$ is the 'quasielastic' Lorentzian with the half-width Γ and $A_0(Q)$ is the elastic incoherent structure factor (EISF). The relative intensity of the 'quasielastic' component is found to increase with increasing Q, its half-width Γ being nearly Q-independent. These features are typical of the case of spatially confined (localized) motion [15]. The value of Γ is proportional to the hydrogen hopping rate τ_l^{-1}, and $A_0(Q)$ contains information on the geometry of localized motion [15]. Thus, our measurements have revealed the existence of a localized H motion in both C15- and C14-type $ZrCr_2H_x$ with the characteristic hopping rates being within the frequency 'window' of the backscattering spectrometers for 128 K $\leqslant T \leqslant$ 173 K.

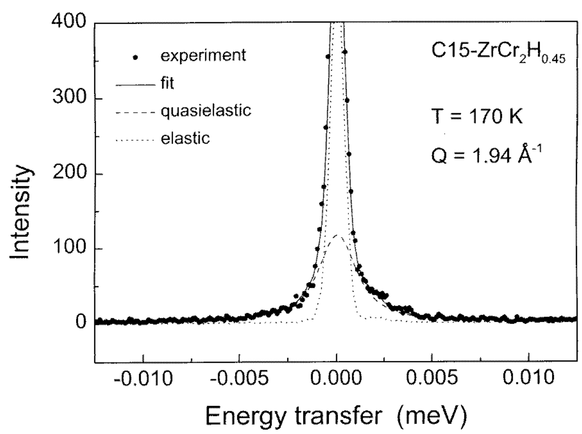

Figure 1. The quasielastic neutron scattering spectrum for C15-$ZrCr_2H_{0.45}$ measured on IN10 at 170 K and $Q = 1.94$ Å^{-1}. The solid curve shows the fit of the two-component model to the data. The dotted curve represents the spectrometer resolution function (the 'elastic' component), and the dashed curve shows the Lorentzian 'quasielastic' component.

Above 200 K the effects of the long-range H diffusion become observable. In this temperature range the hopping rate of the localized H motion is higher than the frequency 'window' of the backscattering spectrometers; therefore, instead of the low-temperature 'quasielastic' curve we observe a flat background. As expected, this background is Q-dependent, increasing with increasing Q. On the other hand, the low-temperature 'elastic' curve shows a pronounced broadening above 200 K. In this range the QENS spectra can be reasonably described by a sum of a flat background and a single Lorentzian convoluted with the instrumental resolution function. The observed Q-dependence of the half-width Γ_0 of this Lorentzian is typical of the case of jump diffusion [15]. For parametrization of the $\Gamma_0(Q)$ dependence we have used the orientationally averaged Chudley–Elliott model [16] describing the diffusion with the constant jump length L and with random distribution of jump directions. The values of Γ_0 are found to increase with increasing temperature. Above room temperature the fitting of the QENS spectra at high Q becomes problematic, since the corresponding values of Γ_0 are comparable to the energy-transfer 'window' of the backscattering spectrometers.

Thus the extremely high hydrogen mobility in $ZrCr_2$ allows us to probe both the localized H motion and the long-range H diffusion below room temperature. In the following sections we shall discuss the parameters of these two types of H motion.

3.2. Localized hydrogen motion

As noted above, in the temperature range 128–173 K the observed QENS spectra for both C15- and C14-type compounds can be satisfactorily described in terms of equation (1) with a nearly Q-independent half-width Γ. In order to assess Γ and $A_0(Q)$ at each temperature, we have used a simultaneous fit of $S_{\text{inc}}(Q, \omega)$ to the data at all Q with a common value of Γ.

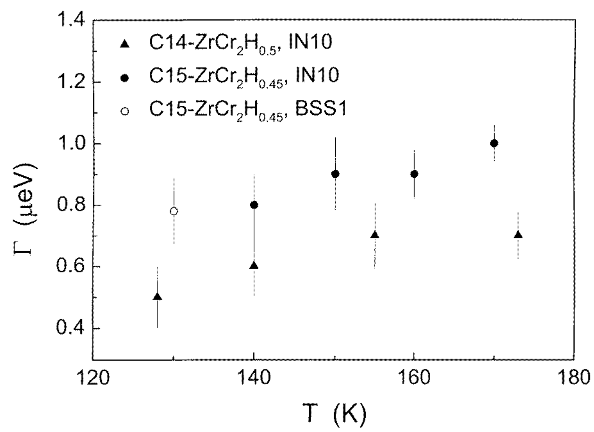

Figure 2. The temperature dependence of the half-width (HWHM) of the 'quasielastic' curve for C14-$ZrCr_2H_{0.5}$ and C15-$ZrCr_2H_{0.45}$, as measured on IN10 and BSS1.

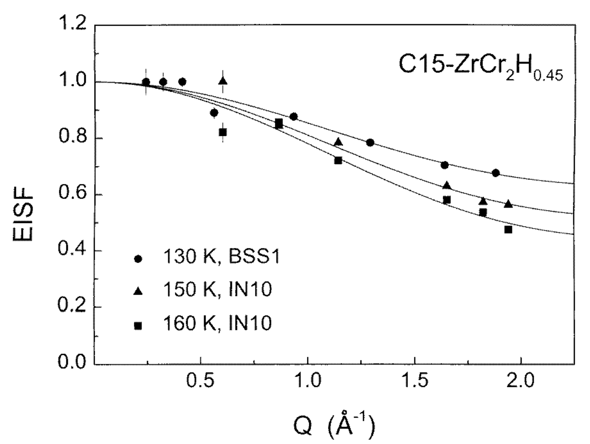

Figure 3. The elastic incoherent structure factor for C15-$ZrCr_2H_{0.45}$ as a function of Q at $T = 130$, 150 and 160 K. The solid curves represent the fits of the six-site model (equation (2)) with fixed $r = 1.13$ Å to the data.

The temperature dependence of the fitted quasielastic half-width Γ for C15-$ZrCr_2H_{0.45}$ and C14-$ZrCr_2H_{0.5}$ is shown in figure 2. It can be seen that the half-width tends to increase with increasing temperature, the values of Γ for the C15-type compound being somewhat higher than the corresponding values for the C14-type compound. Figures 3 and 4 show the behaviour of the elastic incoherent structure factor $A_0(Q)$ at a number of temperatures for C15-$ZrCr_2H_{0.45}$ and C14-$ZrCr_2H_{0.5}$, respectively. The measured EISF appears to be temperature dependent, decreasing with increasing T. A similar feature has been found for the EISF in TaV_2H_x [7–9]. In order to account for this feature, we have to assume that only a fraction p of the H atoms participates in the fast localized motion, and this fraction increases with temperature. The fraction $1 - p$ of the 'static' protons (on the frequency scale determined by the spectrometer resolution) contributes only to the 'elastic' curve and makes the observed values of $A_0(Q)$ higher than those expected in the case of $p = 1$. The existence of 'static' protons may result from the H–H interaction leading to the formation of some ordered atomic configurations at low temperatures. In fact, neutron diffraction measurements [12, 17] have revealed the long-range ordering of D in C15-$ZrCr_2D_x$ with x as low as 0.7 at $T < 100$ K. The heat capacity data for C15-$ZrCr_2H_x$ (C15-$ZrCr_2D_x$) with $0.45 \leqslant x \leqslant 0.50$ [18] are also consistent with the H (D) ordering near 70 K. At higher temperatures a short-range order is likely to exist. With increasing T it tends to disappear, resulting in the observed growth of the fraction p.

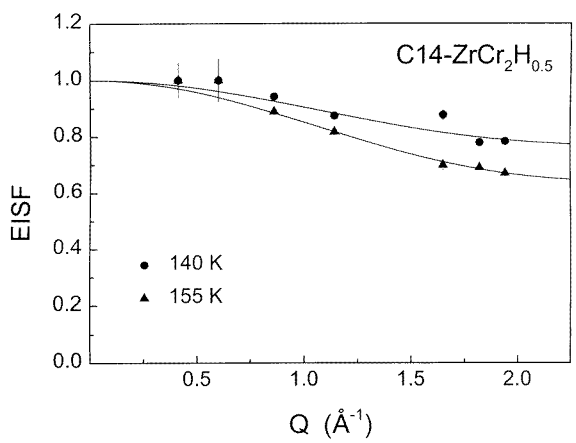

Figure 4. The elastic incoherent structure factor for C14-$ZrCr_2H_{0.5}$ as a function of Q at $T = 140$ and 155 K. The solid curves represent the fits of the six-site model (equation (2)) with fixed $r = 1.16$ Å to the data.

In order to elucidate the geometry of the localized motion, we have to consider the spatial arrangement of the interstitial sites occupied by hydrogen in C15- and C14-type $ZrCr_2$. The structure of the network of interstitial g sites in the C15 lattice has been discussed in detail in our previous papers (see, e.g., figures 5 and 6 of reference [9]). The sublattice of g sites consists of hexagons, the distance r_1 between the nearest sites within the hexagon being shorter than the distance r_2 between the nearest sites on different hexagons. A hydrogen atom moving on such a sublattice is expected to perform many jumps within a hexagon before jumping to the other hexagon. The exact values of r_1 and r_2 depend on the positional parameters of hydrogen atoms at g sites. Using the experimental positional parameters of D atoms at g sites in C15-$ZrCr_2D_{0.7}$ ($X = 0.066$, $Z = 0.872$) [17] to calculate g–g distances in C15-$ZrCr_2H_{0.45}$, we obtain $r_1 = 1.13$ Å, $r_2 = 1.21$ Å.

Let us check now whether the localized motion of H atoms on the g-site hexagons is consistent with the observed Q-dependence of the EISF. In the case where $p \neq 1$, the elastic incoherent structure factor for the model of hopping between six sites on a circle of radius

r [15] is given by

$$A_0(Q,T) = 1 - p(T) + \tfrac{1}{6}p(T)[1 + 2J_0(Qr) + 2J_0(Qr\sqrt{3}) + J_0(2Qr)] \quad (2)$$

where $J_0(x)$ is the Bessel function of zeroth order. The fit of equation (2) to the $A_0(Q)$ data for C15-$ZrCr_2H_{0.45}$ at 160 K yields $p = 0.66 \pm 0.04$, $r = 1.07 \pm 0.06$ Å. The fitted value of r is close to the value $r = r_1 = 1.13$ Å resulting from the structure. By fixing the value of r to 1.13 Å, we have found reasonable fits of the six-site model (equation (2)) to the data at all temperatures in the range 130–170 K with p as the only fit parameter. The results of these fits are shown as solid curves in figure 3. The temperature dependence of p resulting from these fits is shown in figure 5.

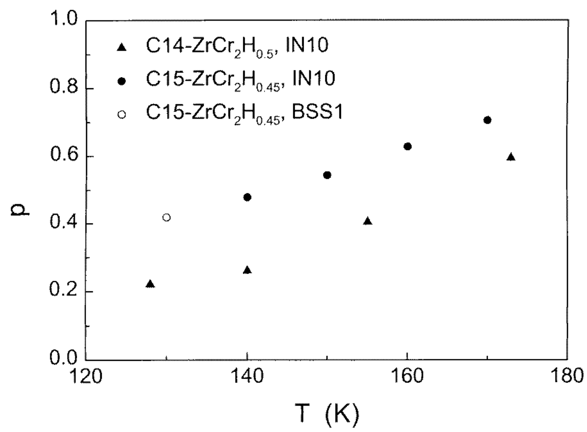

Figure 5. The temperature dependence of the fraction of protons participating in the fast localized motion, as determined from the fits of the six-site model to the data for C14-$ZrCr_2H_{0.5}$ and C15-$ZrCr_2H_{0.45}$.

A more rigorous approach to the data analysis implies a simultaneous fit of $S_{inc}(Q,\omega)$ for the six-site model with fixed $r = 1.13$ Å to the spectra at all Q. Taking into account that only a fraction p of protons participates in the fast localized motion, $S_{inc}(Q,\omega)$ for the six-site model [15] can be written in the form

$$S_{inc}(Q,\omega) = A_0(Q)\delta(\omega) + p\sum_{i=1}^{3} A_i(Q)L(\omega,\Gamma_i) \quad (3)$$

where $A_0(Q)$ is given by equation (2), $L(\omega,\Gamma_i)$ is the Lorentzian function with the half-width Γ_i, $\Gamma_1 = 0.5\tau_l^{-1}$, $\Gamma_2 = 1.5\tau_l^{-1}$, $\Gamma_3 = 2\tau_l^{-1}$ and τ_l is the mean time between two successive jumps of a proton within a hexagon. Thus, for the six-site model the quasielastic curve is expected to consist of three Lorentzian components with different half-widths Γ_i and Q-dependent amplitudes $A_i(Q)$, and the half-width of the composite quasielastic curve should show a certain Q-dependence, especially at $Qr \geqslant 1.5$ [15]. However, as has been noted previously [19], because of the limited experimental accuracy it is difficult to distinguish between such a three-component quasielastic curve and a single Lorentzian with a Q-independent width in the case of a rather weak quasielastic curve coexisting with a strong elastic one. In fact, we have found that the quality of simultaneous fits based on equation (3) with the fit parameters τ_l^{-1} and p is comparable to the quality of simultaneous fits based on equations (1) and (2) with a common Γ. Moreover, the values of p obtained from these two types of fit are nearly the same, and the common Γ-value appears to be close to $0.6\tau_l^{-1}$.

The spatial arrangement of the tetrahedral (Zr_2Cr_2) sites in C14-$ZrCr_2$ is shown in figure 6. As in the case of the C15 structure, the sublattice of (Zr_2Cr_2) sites consists of hexagons; however, these hexagons are formed by inequivalent sites. Type I hexagons are in the basal plane; they are formed by alternating h_1 and h_2 sites. Type II hexagons are formed by two k and

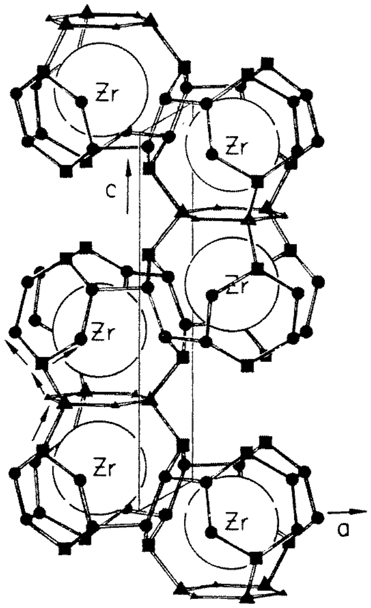

Figure 6. The spatial arrangement of interstitial (Zr_2Cr_2) sites in C14-type $ZrCr_2$ (from [14]). Large triangles: h_1 sites; small triangles: h_2 sites; squares: k sites; solid circles: l sites; large open circles: Zr atoms.

four l sites in the sequence k–l–l–k–l–l. In order to calculate the intersite distances, we have used the actual lattice parameters a_0 and c_0 of C14-$ZrCr_2H_{0.5}$ and the positional parameters of D atoms in h_1, h_2, k and l sites found for the related compound $ZrMn_2D_3$ [14]. The following distances between the nearest neighbours have been obtained:

(a) h_1–h_2 (within type I hexagons): $r_3 = 1.16$ Å;
(b) l–l (within type II hexagons): $r_4 = 1.11$ Å;
(c) k–l (within type II hexagons): $r_5 = 1.19$ Å;
(d) h_1–k (between type I and type II hexagons): $r_6 = 1.23$ Å;
(e) l–l (between two type II hexagons): $r_7 = 1.24$ Å.

Since the distances between the nearest sites within the hexagons (r_3, r_4, r_5) are shorter than the distances between the nearest sites on different hexagons (r_6, r_7), we may again expect that the localized H motion occurs within the hexagons.

If we neglect the small difference between type I and type II hexagons, the Q-dependence of the EISF can still be described in terms of equation (2). The fit of equation (2) to the $A_0(Q)$ data for C14-$ZrCr_2H_{0.5}$ at 155 K yields $p = 0.41 \pm 0.03$, $r = 1.15 \pm 0.07$ Å. Again, the fitted value of r is close to the weighted average of r_3, r_4 and r_5, $\bar{r} = 1.16$ Å. By fixing the value of r to 1.16 Å, we have found reasonable fits of the six-site model (equation (2)) to the data at all temperatures in the range 128–173 K with p as the only fit parameter. The results of these fits are shown as solid curves in figure 4. The temperature dependence of p resulting from these fits is included in figure 5. Comparison of the $p(T)$ results for C15-$ZrCr_2H_{0.45}$ and C14-$ZrCr_2H_{0.5}$ shows that for the same temperature the fraction of H atoms participating in the fast localized motion in the C14-type compound is considerably lower than for the C15 counterpart. It should be noted, however, that the apparent p-value for the C14 compound can be affected by the difference between intersite distances r_4 and r_5 within type II hexagons. In fact, this difference is expected to lead to a difference between H residence times in k and l sites forming type II hexagons. Such an asymmetry results in an increase in $A_0(Q)$ with respect to that for the symmetric case [15]; as has been discussed in [7], it is practically impossible to distinguish this $A_0(Q)$ increase from that caused by a decrease in p.

The usual approach to the description of $p(T)$ is based on the assumption of a certain energy gap ΔE between 'static' and 'mobile' H states (see, e.g., [20]). In this case,

$$p(T) = \frac{b_m \exp(-\Delta E/k_B T)}{1 + b_m \exp(-\Delta E/k_B T)} \qquad (4)$$

where b_m is the relative degeneracy factor of 'mobile' states. However, even in a rather narrow temperature range of the available $p(T)$ data we have not been able to get a satisfactory description of the experimental results using equation (4). As in the case of TaV_2H_x [9], this may indicate the existence of a broad ΔE distribution resulting from a spread in local H configurations.

3.3. Long-range diffusion of hydrogen

As noted in section 3.1, above 200 K the experimental QENS spectra for both C15- and C14-type compounds can be satisfactorily described by a sum of a flat background and a single Lorentzian convoluted with the instrumental resolution function. The Q-dependence of the half-width Γ_0 of this Lorentzian is typical of the case of jump diffusion. At low Q

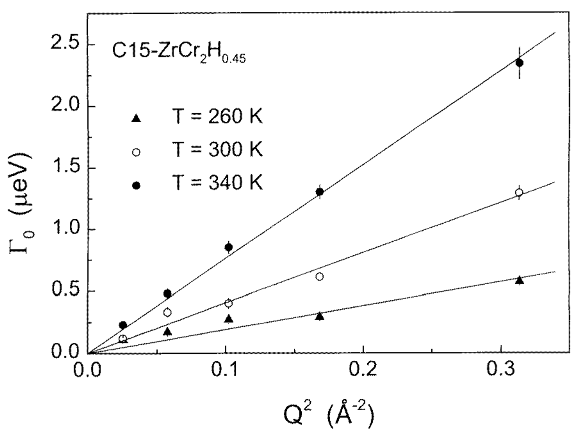

Figure 7. The half-width (HWHM) of the diffusion-broadened Lorentzian quasielastic curve as a function of Q^2 in the low-Q range for $T = 260$, 300 and 340 K. The solid lines show the fits of equation (5) to the data.

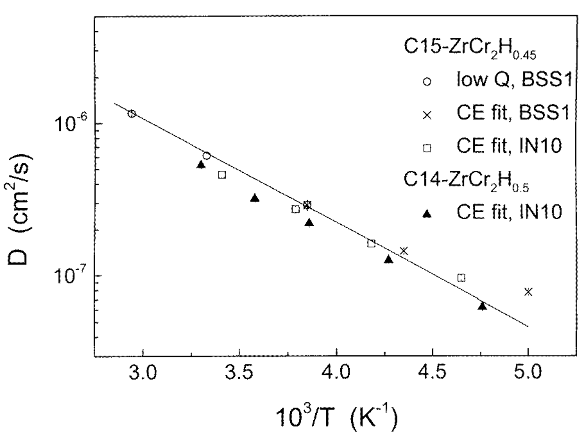

Figure 8. The temperature dependence of the tracer diffusion coefficient of hydrogen in C15-$ZrCr_2H_{0.45}$ and C14-$ZrCr_2H_{0.5}$, as determined from the low-Q data (equation (5)) and from the Chudley–Elliott fits. The solid line shows the Arrhenius fit of the D-values derived from the low-Q data for C15-$ZrCr_2H_{0.45}$.

(corresponding to $QL \ll 1$) the value of Γ_0 is expected to be proportional to Q^2 [15]:

$$\Gamma_0 = \hbar D Q^2 \tag{5}$$

where D is the tracer diffusion coefficient for hydrogen. The low-Q range has been studied only for C15-$ZrCr_2H_{0.45}$ in the measurements on BSS1. Figure 7 shows the observed behaviour of Γ_0 as a function of Q^2 for three temperatures. Below 260 K the line broadening at low Q is too small to be reliably determined with the available instrumental resolution. As can be seen from figure 7, in the range 260–340 K the Q-dependence of Γ_0 at low Q is reasonably well described by equation (5). The values of the diffusion coefficient resulting from the corresponding fits are shown by open circles in figure 8. These model-independent values appear to be about a factor of 2 higher than those obtained from the pulsed-field-gradient (PFG) NMR measurements [3] for C15-$ZrCr_2H_{0.5}$. However, the activation energy E_a^D for H diffusion found from our D-data over the range 260–340 K (136 ± 5 meV) is in excellent agreement with that derived from the PFG-NMR results [3] above 200 K (137 meV).

Examples of the dependence $\Gamma_0(Q)$ over the entire Q-range studied are shown in figures 9 and 10. For parametrization of this dependence we have used the orientationally averaged Chudley–Elliott model [16]. The corresponding form of $\Gamma_0(Q)$ is

$$\Gamma_0(Q) = \frac{\hbar}{\tau_d}\left(1 - \frac{\sin QL}{QL}\right) \tag{6}$$

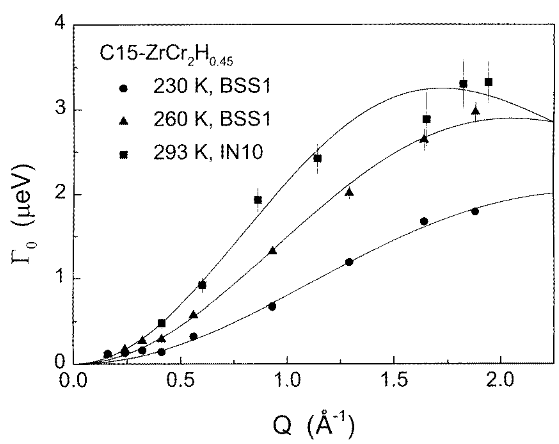

Figure 9. The half-width of the Lorentzian QENS component for C15-$ZrCr_2H_{0.45}$ as a function of Q at $T = 230$, 260 and 293 K. The solid curves show the fits of the Chudley–Elliott model (equation (6)) to the data.

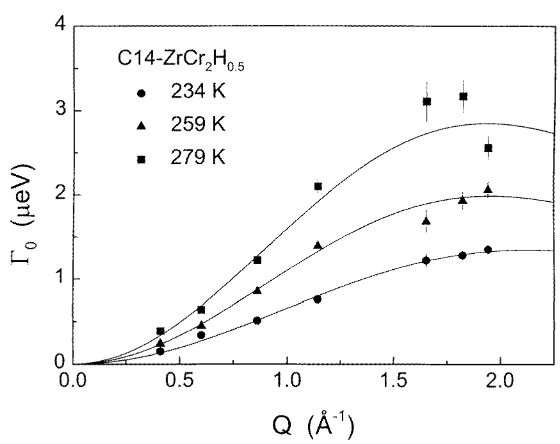

Figure 10. The half-width of the Lorentzian QENS component for C14-$ZrCr_2H_{0.5}$ as a function of Q at $T = 234$, 259 and 279 K. The solid curves show the fits of the Chudley–Elliott model (equation (6)) to the data.

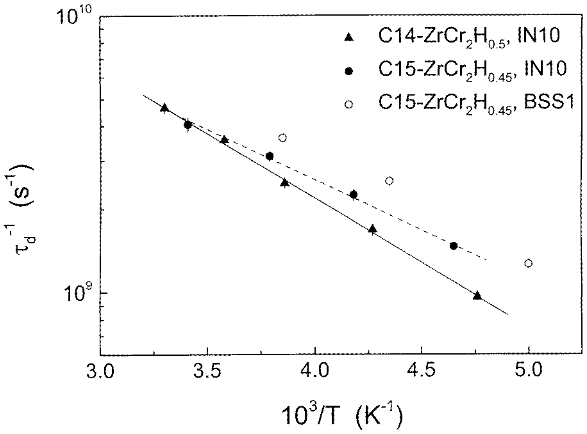

Figure 11. The temperature dependence of the hydrogen hopping rate τ_d^{-1} derived from the Chudley–Elliott fits (equation (6)). The solid line shows the Arrhenius fit to the data for C14-$ZrCr_2H_{0.5}$. The dashed line represents the Arrhenius fit to the IN10 data for C15-$ZrCr_2H_{0.45}$.

where τ_d is the mean time between two successive H jumps leading to long-range diffusion. The fits of equation (6) to the data are shown by the solid curves in figures 9 and 10. The temperature dependences of τ_d^{-1} resulting from the Chudley–Elliott fits for C15-$ZrCr_2H_{0.45}$ and C14-$ZrCr_2H_{0.5}$ are presented in figure 11. As can be seen from this figure, for both C15- and C14-type compounds the behaviour of τ_d^{-1} is reasonably well described by the Arrhenius law:

$$\tau_d^{-1} = \tau_{d0}^{-1} \exp(-E_a^\tau / k_B T). \tag{7}$$

There is a small difference between the τ_d^{-1}-values for C15-$ZrCr_2H_{0.45}$ resulting from the measurements on IN10 and BSS1; only the Arrhenius fit for the IN10 data is shown in figure 11. The fitted values of τ_{d0}^{-1} are $(7.5\pm1.0)\times10^{10}$ s^{-1} and $(1.6\pm0.1)\times10^{11}$ s^{-1} for the C15- and C14-type compounds, respectively. The activation energies E_a^τ resulting from the Arrhenius fits are 73 ± 3 meV (C15) and 93 ± 2 meV (C14). For C15-$ZrCr_2H_{0.45}$ the values of τ_{d0}^{-1} and E_a^τ can be compared to those derived from the NMR measurements of the proton spin–lattice relaxation rate in C15-$ZrCr_2H_{0.5}$ [2], $\tau_{d0}^{-1} = 5.5 \times 10^{10}$ s^{-1}, and the average activation energy $\bar{E}_a = 84$ meV. The agreement between the QENS and the NMR relaxation results for τ_d^{-1} appears to be satisfactory. It should be noted, however, that the activation energy E_a^τ describing the temperature dependence of τ_d^{-1} is considerably lower than the activation energy E_a^D for the tracer diffusion coefficient D. We shall return to the discussion of this unusual feature below.

The values of the effective jump length L resulting from the Chudley–Elliott fits show systematic increase with increasing temperature. For C15-$ZrCr_2H_{0.45}$ the fitted L-value is found to change from 1.92 ± 0.06 Å at 200 K to 2.6 ± 0.1 Å at 293 K; for C14-$ZrCr_2H_{0.5}$ it grows from 1.97 ± 0.07 Å at 210 K to 2.62 ± 0.09 Å at 303 K. Note that the effective jump length is always considerably longer than the distance between the nearest (Zr_2Cr_2) sites on different hexagons ($r_2 = 1.21$ Å for C15-$ZrCr_2H_{0.45}$ and $r_6 = 1.23$ Å, $r_7 = 1.24$ Å for C14-$ZrCr_2H_{0.5}$). The values of L exceeding 2 Å have also been reported previously for a number of cubic Laves phase hydrides with g-site occupation [3, 9, 21, 22]. This feature can be naturally explained in terms of our model implying two frequency scales of H motion: the rate of hopping within hexagons (τ_l^{-1}) and the rate of hopping between hexagons (τ_d^{-1}) with $\tau_d^{-1} \ll \tau_l^{-1}$. In this model, τ_d is the mean residence time of a hydrogen atom *at a hexagon* (not at an interstitial site, as usually). Since a H atom may enter a hexagon through one site and leave it from the other site, the total displacement for the time τ_d is the distance between the nearest sites on different hexagons plus the additional displacement between the initial and the final positions of a hydrogen atom at the hexagon. Both the half-width Γ_0 and the maximum of the spin–lattice relaxation rate in NMR experiments are determined by the slower frequency scale τ_d^{-1}; therefore the apparent jump length L derived from these measurements is considerably longer than the distance between the nearest (Zr_2Cr_2) sites on different hexagons.

The observed growth of L with increasing temperature may be related to increasing fraction of H atoms participating in the fast localized motion. In fact, if a hydrogen does not participate in the localized motion on the timescale of τ_l, its displacement for time τ_d is expected to be shorter than that of H atoms participating in the localized motion. Therefore the increase in p leads to the shift of the distribution of individual displacements for time τ_d to higher values; this results in the growth of the effective L-value.

The relation between the tracer diffusion coefficient D and the values of τ_d and L is given by

$$D = \frac{L^2}{6\tau_d}. \tag{8}$$

We assume here that the tracer correlation factor [23] for H diffusion is equal to 1. This assumption is well justified, since in our $ZrCr_2H_x$ samples less than 5% of all available tetrahedral sites are occupied by hydrogen. Using the values of τ_d and L derived from the Chudley–Elliott fits, we can obtain D from equation (8). The resulting D-values are included in figure 8. Note that for C15-$ZrCr_2H_{0.45}$ the three sets of D-values (determined from the low-Q data and from the Chudley–Elliott fits of the BSS1 and IN10 data) are in good agreement. At $T \geqslant 215$ K all of these data sets can be characterized by the activation energies E_a^D over the range 125–140 meV, in agreement with the PFG-NMR results [3]. As noted above, these E_a^D-values are considerably higher than the activation energy E_a^τ for τ_d derived from the proton spin–lattice relaxation rate [2] and from the present QENS measurements (70–85 meV for the C15-type compound). The origin of this difference can be understood, if we take into account the observed temperature dependence of L. Since the effective jump length is found to increase with increasing temperature, it follows from equation (8) that D grows with temperature faster than τ_d^{-1}, at least in the range where L is temperature dependent. This feature results from the specific mechanism of H diffusion in Laves phase compounds implying two frequency scales of hydrogen hopping and the temperature-dependent fraction of H atoms participating in the faster motion.

As can be seen from figure 8, the temperature dependence of D over the range 200–340 K shows a small deviation from the Arrhenius behaviour. Much stronger deviations from the Arrhenius behaviour of D below 200 K were observed in the PFG-NMR experiments for both C14- and C15-type $ZrCr_2H_x$ [3]. Although temperature dependence of L can contribute to the observed deviations, the changes in the slope of Arrhenius plots of D found by PFG-NMR [3] are too strong to be attributed solely to changes in L. This means that a change in the physical mechanism of elementary H jumps is likely to occur in $ZrCr_2H_x$ below 200 K.

3.4. Comparison with the results for C15-type TaV_2H_x

In order to discuss the systematics of H motion in cubic Laves phase compounds, it is useful to compare the QENS results for C15-$ZrCr_2H_{0.45}$ with those for C15-TaV_2H_x [9]. The microscopic picture of hydrogen diffusion in C15-$ZrCr_2H_{0.45}$ appears to be qualitatively the same as for C15-TaV_2H_x. However, there is a substantial difference between the motional parameters of hydrogen in these compounds. The localized H motion in $ZrCr_2$ is slower, whereas the long-range diffusion is much faster than in TaV_2. Therefore the two frequency scales of H motion in $ZrCr_2$ are much closer to each other than in TaV_2.

It has been suggested [9] that in cubic Laves phases the hydrogen hopping rates τ_l^{-1} and τ_d^{-1} strongly depend on the distances r_1 and r_2, respectively (the decrease in the distances leads to the increase in the corresponding hopping rates). In its turn, the ratio r_2/r_1 is believed to be determined by the ratio of metallic radii R_A/R_B of the elements A and B forming the AB_2 intermetallic [9]. Table 1 shows the values of R_A/R_B, the structural parameters and the parameters of hydrogen motion in C15-type $ZrCr_2H_{0.45}$ and $TaV_2H_{0.6}$. The positional parameters of hydrogen at g sites, X and Z, in $ZrCr_2$ and TaV_2 are determined from the neutron diffraction measurements on $ZrCr_2D_{0.7}$ [17] and TaV_2D_x [24], respectively; the g–g distances r_1 and r_2 are calculated using these positional parameters. The values of τ_l^{-1}(140 K), τ_d^{-1}(320 K) and D(320 K) for $ZrCr_2H_{0.45}$ are the results from the present work, and the value of τ_l^{-1}(140 K) for $TaV_2H_{0.6}$ is taken from reference [9]. Since for the TaV_2H_x system QENS measurements probing the long-range diffusion have been performed only on the sample with $x = 1.1$ [9], the actual values of τ_d^{-1}(320 K) and D(320 K) included in table 1 relate to $TaV_2H_{1.1}$. From the NMR experiments [5] it is known that in TaV_2H_x the value of τ_d^{-1} slowly increases with increasing x.

Table 1. The ratio of metallic radii of the elements A and B forming the AB_2 intermetallic, the structural parameters and the parameters of H motion in C15-type $ZrCr_2H_{0.45}$ and $TaV_2H_{0.6}$.

Parameter	$ZrCr_2H_{0.45}$	$TaV_2H_{0.6}$
R_A/R_B	1.250	1.090
X	0.066	0.055
Z	0.872	0.888
a_0 (Å)	7.26	7.22
r_1 (Å)	1.13	0.99
r_2 (Å)	1.21	1.44
r_2/r_1	1.07	1.45
τ_l^{-1}(140 K) (s^{-1})	3.2×10^8	6.5×10^9
τ_d^{-1}(320 K) (s^{-1})	4.2×10^9	2.2×10^8
D(320 K) ($cm^2\ s^{-1}$)	8.6×10^{-7}	3.8×10^{-8}

Although the lattice parameters a_0 of $ZrCr_2H_{0.45}$ and $TaV_2H_{0.6}$ are close to each other, there is a considerable difference between the g–g distances in these compounds. As can be seen from table 1, for $ZrCr_2H_{0.45}$ the r_1-value is longer and the r_2-value is shorter than in $TaV_2H_{0.6}$. The difference is especially pronounced for the ratio r_2/r_1. The structural data presented in table 1 indicate the possibility of large variations of this ratio characterizing the sublattice of g sites in cubic Laves phases. This means that, depending on positional parameters X and Z in different Laves phases, the g-site hexagons may be well or poorly separated from each other. It is known that for many intermetallic hydrides the hydrogen–metal distances are nearly the same as in the corresponding metal hydrides [12, 13]. Therefore one may expect the positional parameters of hydrogen in interstitial sites formed by different metal atoms (A_2B_2 in the case of g sites) to depend on R_A/R_B. The 'ideal' value of R_A/R_B for Laves phase compounds (corresponding to the closest packing of hard spheres) is 1.225, the resulting 'ideal' values of the positional parameters of hydrogen, X_{id} and Z_{id}, being equal to 0.063 and 0.875, respectively. It can be seen from table 1 that for the $ZrCr_2$–H system both R_A/R_B and the positional parameters of hydrogen are close to the corresponding 'ideal' values, whereas for TaV_2–H there are strong deviations of both R_A/R_B and the positional parameters X and Z from their 'ideal' values. In general, we expect that the highest r_2/r_1 ratio should be found in Laves phases with the lowest R_A/R_B. The difference between r_1 and r_2 is expected to disappear with increasing R_A/R_B.

Comparison of the hydrogen hopping rates presented in table 1 shows that for $ZrCr_2H_{0.45}$ the value of τ_l^{-1}(140 K) is considerably lower and the value of τ_d^{-1}(320 K) is higher than the corresponding values for $TaV_2H_{0.6}$. The smaller difference between the two frequency scales of H motion in $ZrCr_2$ is consistent with the smaller r_2/r_1 ratio. NMR measurements of the proton spin–lattice relaxation rate T_1^{-1} in TaV_2H_x [5] have revealed two maxima in $T_1^{-1}(T)$. The main high-temperature maximum (290–360 K) is determined by the condition $\omega_H \tau_d \approx 1$, and the low-temperature maximum corresponds to $\omega_H \tau_l \approx 1$, where ω_H is the nuclear magnetic resonance frequency for protons. For $ZrCr_2H_x$ the additional low-temperature maximum of the spin–lattice relaxation rate is not observed [2] because of the smaller difference between the two frequency scales of H motion. However, the localized H motion in $ZrCr_2H_x$ contributes to the change in the low-temperature slope of the dependence $T_1^{-1}(T)$ and to the reduction of the amplitude of the maximum in $T_1^{-1}(T)$ [2]. In fact, the maximum T_1^{-1}-value is determined by the mean square strength $\langle M^2 \rangle$ of the fluctuating internuclear dipole–dipole interaction [25], but at the temperature of the relaxation rate maximum, T_{max}, a certain part of $\langle M^2 \rangle$ appears to be averaged out by the fast localized H motion. This part should be proportional to $p(T_{max})$. Since p increases with temperature, one may expect that the reduction of the relaxation rate maximum is stronger for higher T_{max}-values. This is consistent with the results of recent NMR measurements [26] of the rotating-frame spin-relaxation rate $T_{1\rho}^{-1}$ in $ZrCr_2H_x$ $(0.2 \leqslant x \leqslant 0.5)$. The T_{max}-values for $T_{1\rho}^{-1}$ are much lower than for T_1^{-1}, since the $T_{1\rho}^{-1}$-maximum is determined by the condition $\omega_1 \tau_d \approx 1$, where the nutation frequency ω_1 is at least two orders of magnitude lower than the resonance frequency ω_H. It has been found [26] that the maximum values of $T_{1\rho}^{-1}$ in $ZrCr_2H_x$ are higher than those expected on the basis of the T_1^{-1}-data in the same samples. This can be qualitatively explained in terms of the temperature-dependent fraction p: because of the increase in p with increasing temperature, the localized H motion leads to a slight reduction of the $T_{1\rho}^{-1}$-maximum and to a stronger reduction of the T_1^{-1}-maximum.

4. Conclusions

The analysis of our quasielastic neutron scattering data for C15-$ZrCr_2H_{0.45}$ and C14-$ZrCr_2H_{0.5}$ has shown that in both systems the diffusive motion of hydrogen can be described in terms of at least two jump processes with different frequency scales. The faster process implies H jumps within the hexagons formed by interstitial (Zr_2Cr_2) sites; this localized motion is characterized by the hopping rate τ_l^{-1}. The slower process with the hopping rate τ_d^{-1} corresponds to jumps from one hexagon to the other. It is found that only a fraction p of H atoms participates in the fast localized motion, and this fraction increases with temperature. The motional parameters of hydrogen in the C15- and C14-type samples are found to be close to each other, the values of τ_l^{-1} and τ_d^{-1} for C15-$ZrCr_2H_{0.45}$ being slightly higher than the corresponding values for C14-$ZrCr_2H_{0.5}$.

The hydrogen diffusion coefficients D obtained from the low-Q QENS data and from the Chudley–Elliott model in the range 200–340 K can be reasonably described by the Arrhenius law with the activation energy $E_a^D \approx 0.13$ eV. However, this value appears to be considerably higher than the activation energy E_a^τ ($\sim$0.07 eV for the C15-type sample) describing $\tau_d^{-1}(T)$ over the same temperature range. The inequality $E_a^\tau < E_a^D$ as well as the high values of the apparent jump length of H atoms are shown to result from the specific microscopic picture of hydrogen diffusion implying two frequency scales of H hopping and the temperature-dependent fraction of atoms participating in the faster motion.

Comparison of the motional parameters of hydrogen in the cubic Laves phases $ZrCr_2$ and TaV_2 shows that the localized H motion in $ZrCr_2$ is slower, whereas the long-range H diffusion is much faster than in TaV_2. Therefore, the two frequency scales of H motion in $ZrCr_2$ are much closer to each other than in TaV_2. This is consistent with the small difference between the intersite g–g distances r_1 and r_2 in $ZrCr_2H_x$. Our results also support the idea [9] that the ratio r_2/r_1 is related to the ratio R_A/R_B of metallic radii of the elements forming a cubic Laves phase AB_2. In order to verify the relation between the H hopping rates, the g–g distances and R_A/R_B, it is necessary to determine both the positional parameters of hydrogen at g sites and the hopping rates τ_l^{-1} and τ_d^{-1} in a number of Laves phases with different values of R_A/R_B. Such a study is in progress now.

Acknowledgments

This work was partially supported by the Russian Foundation for Basic Research (grant 96-02-16517). AVS acknowledges financial support of the Alexander von Humboldt Foundation and Universität des Saarlandes.

References

[1] Skripov A V, Belyaev M Yu and Stepanov A P 1991 *Solid State Commun.* **78** 909
[2] Skripov A V and Belyaev M Yu 1993 *J. Phys.: Condens. Matter* **5** 4767
[3] Renz W, Majer G, Skripov A V and Seeger A 1994 *J. Phys.: Condens. Matter* **6** 6367
[4] Bowman R C, Craft B D, Attalla A and Johnson J R 1983 *Int. J. Hydrogen Energy* **8** 801
[5] Skripov A V, Rychkova S V, Belyaev M Yu and Stepanov A P 1990 *J. Phys.: Condens. Matter* **2** 7195
[6] Skripov A V, Belyaev M Yu, Rychkova S V and Stepanov A P 1991 *J. Phys.: Condens. Matter* **3** 6277
[7] Skripov A V, Cook J C, Karmonik C and Hempelmann R 1996 *J. Phys.: Condens. Matter* **8** L319
[8] Skripov A V, Cook J C, Karmonik C and Hempelmann R 1997 *J. Alloys Compounds* **253+254** 432
[9] Skripov A V, Cook J C, Sibirtsev D S, Karmonik C and Hempelmann R 1998 *J. Phys.: Condens. Matter* **10** 1787
[10] Fruchart D, Rousault A, Shoemaker C B and Shoemaker D P 1980 *J. Less-Common Met.* **73** 363
[11] Yartys V A, Burnasheva V V, Fadeeva N V, Solov'ev S P and Semenenko K N 1980 *Dokl. Akad. Nauk SSSR* **255** 582
[12] Somenkov V A and Irodova A V 1984 *J. Less-Common Met.* **101** 481
[13] Yvon K and Fischer P 1988 *Hydrogen in Intermetallic Compounds I* ed L Schlapbach (Berlin: Springer) p 87
[14] Didisheim J J, Yvon K, Shaltiel D and Fischer P 1979 *Solid State Commun.* **31** 47
[15] Bée M 1988 *Quasielastic Neutron Scattering* (Bristol: Hilger)
[16] Chudley C T and Elliott R J 1961 *Proc. Phys. Soc.* **77** 353
[17] Fischer P, Fauth F, Skripov A V and Kozhanov V N 1999 to be published
[18] Skripov A V, Karkin A E and Mirmelstein A V 1997 *J. Phys.: Condens. Matter* **9** 1191
[19] Schönfeld C, Hempelmann R, Richter D, Springer T, Dianoux A J, Rush J J, Udovic T J and Bennington S M 1994 *Phys. Rev.* B **50** 853
[20] Berk N F, Rush J J, Udovic T J and Anderson I S 1991 *J. Less-Common Met.* **172–174** 496
[21] Schönfeld C 1992 *PhD Thesis* Technische Hochschule Aachen
[22] Havill R L, Titman J M, Wright M S and Crouch M A 1989 *Z. Phys. Chem., NF* **164** 1083
[23] Tahir-Kheli R A and Elliott R J 1983 *Phys. Rev.* B **27** 844
[24] Fischer P, Fauth F, Skripov A V, Podlesnyak A A, Padurets L N, Shilov A L and Ouladdiaf B 1997 *J. Alloys Compounds* **253+254** 282
[25] Barnes R G 1997 *Hydrogen in Metals III* ed H Wipf (Berlin: Springer) p 93
[26] Stoddard R D and Conradi M S 1998 *Phys. Rev.* B **57** 10 455